

# Current Sensor Fault Reconstruction and Compensation of an AC-Voltage Sensorless Controlled Single Phase Grid Connected Converter using PI-Observers

M.Dardouri\*<sup>‡</sup>, S.Khojet El Khil\*, K.Jelassi\*

\* Université de Tunis El Manar, Ecole Nationale d'Ingénieurs de Tunis, LR11ES15 Laboratoire des Systèmes Électriques, 1002, Tunis, Tunisie

(meriem.dardouri@enit.utm.tn, sejir.kek@edu.isetcom.tn, khaled.jelassi@enit.utm.tn)

<sup>‡</sup>Corresponding Author ; M.Dardouri, Université de Tunis El Manar, Ecole Nationale d'Ingénieurs de Tunis, LR11ES15 Laboratoire des Systèmes Électriques, 1002, Tunis, Tunisie, [meriem.dardouri@enit.utm.tn](mailto:meriem.dardouri@enit.utm.tn)

*Received: 14.01.2022 Accepted: 27.02.2022*

**Abstract-** Ensuring reliability and availability while reducing cost are the main desirable characteristics of single-phase grid connected converters. With a view to guarantee the aforementioned characteristics, this work presents a grid current sensor fault tolerant control (FTC) of an AC voltage sensorless controlled single-phase grid connected converter. Contrary to classical sensor FTC methods based on residual generation, the proposed approach aims to reconstruct the current sensor fault. Hence, a bank of proportional-Integral (PI) observers is proposed to first, insure accurate estimation of the grid voltage and second to achieve a robust grid current sensor fault estimation. Finally, the current sensor fault tolerant control process consists on fault compensation in the converter's control loop as well as in the grid voltage estimation stages. The effectiveness of the proposed FTC algorithm is demonstrated through simulation under Matlab/Simulation Software and experimental results.

**Keywords** Grid Connected Converter, Voltage Sensorless Control, Sensor Fault Estimation, Sensor Fault Compensation, Proportional-Integral Observers.

## 1. Introduction

Single Phase Grid Connected Converters (SPGCC) are today widely used in many areas such as renewable energy sources [1,4], electric railway traction systems [5], EVs [6-7], avionics, industrial production, etc. SPGCC have many advantages such as grid unity power factor operation, grid current sinusoidal waveform and DC-link voltage regulation [5]. As any power converter working with feedback closed loop control, SPGCC needs accurate measurements to reach the wanted performances. For inverter operation of the SPGCC, the conventional closed loop control needs, in addition to the grid current measurement, accurate information of the fundamental of the grid voltage and so one voltage sensor for the grid voltage measurement is employed. In order to reduce the system costs and to increase its reliability, the AC voltage sensor may be removed and the grid voltage is estimated.

Consequently, several grid voltage estimation approaches have been discussed in the literature. Sliding mode observers have been employed to estimate grid voltage for three phase grid connected converters in [8-9],

[12]. In [10-12], virtual flux estimators are presented to insure high performances model predictive control grid connected converters under grid-unbalanced voltages. Model Reference Adaptive System (MRAS) estimators have been also described to estimate grid voltage for single-phase T-type rectifier [13] and three phase inverters [14]. The suggested MRAS estimators are based on grid active and reactive power estimation. The MRAS technique is used in [15] to estimate capacitor voltage for the active damping control of a single-phase grid connected inverter with LCL filter. Finally, extended state observers have been discussed in [16]. Once the grid voltage sensor is removed, the converter's control loop is driven by only the grid current sensor. Unfortunately, current sensors still sensitive to several types of failures that can destroy the SPGCC performances or even cause unplanned shutdown of the SPGCC. Therefore, fault detection and estimation are necessary for the system safe operation. To this end, different sensor fault detection and isolation (FDI) and FTC approaches have been developed in the literature [17-18]. They may be classified in three

categories: model-based [5], [19-22], signal-based [23-26] and data driven, [27-30].

As a traditional approach, model-based methods require the use of the system mathematical model. Then after, estimated quantities are compared to measured ones based on residuals generation. The fault diagnostic is achieved when the generated residuals exceed a predefined thresholds. These methods usually use observers such as state observers [5], [17-20], Kalman Filter [20], Sliding Mode observer (SMO) [21], Model Reference Adaptive System (MRAS) [23] and so on. In [5], a state observer based sensor FDI and FTC of a single-phase pulse width modulated (PWM) rectifier for electric railway traction system is discussed. The presented approach is based on residual generation. When the faulty sensor is identified, the erroneous measurement is substituted by the estimated quantity in the control loop. In [20], authors addressed a fault-tolerant control of a smart PV-grid system. The suggested FTC algorithm deals with the load current sensor failure through the use of two observers: a sliding mode based Luenberger observer and a Kalman filter observer then according to the residue value and via an Euler based voting algorithm the appropriate observer is enabled. In [21], a sliding mode observer (SMO) based algorithm for the fault detection and fault reconfiguration of catenary current and DC-link voltage sensor faults of a single phase PWM rectifier for electric traction applications was developed considering three kinds of sensor faults and unipolar and bipolar modulation methods. In [22], a MRAS based sensors FDI and FTC of three phase inverter for PV system application is developed. Using residual generation and fixed thresholds technique, three FDI algorithms were suggested to detect the fault occurrence in grid voltages, line currents and dc-link voltage sensors.

Regarding the use of signal based methods, several techniques have been presented in the literature. The main advantage of this technique is that, for systems which are hardly mathematically modeled, it extract signal features as diagnostic variable. Hence, signal based method is system's model free. In [23], authors presented a signal-based technique that uses the signs of the detection variables to identify the faulty sensor. In [24], a FPGA-based current sensor fault tolerant control for a three-phase grid connected converter was introduced. The developed control technique ensures the converter's continuous operation even with current sensor fault via hardware redundancy of the current sensor. In [25], a new fault diagnosis method for multiple IGBT and current sensor fault was developed. The suggested approach relies on the stator current analysis and does not need any other information, which ensure robustness and high reliability. In [26], the current sensor FDI was performed by analyzing the three-phase currents.

In addition to model-based and signal-based methods, and thanks to the great advance and development in data analytics techniques, data-driven methods have gained a lot of attention recently. In [27], a hybrid model-based and data driven grid current fault tolerant control for a single-phase PWM rectifier was presented. In [28], for sensor

fault diagnosis, a new feature generation method is developed based on a statistical time-domain. Then, support vector machine (SVM) is applied to learn the historic database and diagnose the practical system online. In [29], authors presented an intelligent method for sensor fault diagnosis in a three-phase PWM inverter fed induction motor drive system, where an emerging machine learning machine (ELM) is applied to learn the sensor fault database. The authors in [30] characterized the system statistical features to ensure a data-driven diagnosis process via monitoring the evolution of the correlation between the system variables.

More recently, fault estimation (FE) and fault compensation approaches have been studied as an alternative effective method to classical FDI-FTC methods [31-35]. The main idea of FE approaches is to estimate the sensor fault (size, shape and so on) [31][32]. The estimated fault is directly used in the system's control loop to compensate the fault effects. Moreover, FE-FTC intrinsically includes fault detection and fault isolation roles without the need of residuals and fault detection thresholds. Hence, FE-FTC offers much more flexibility and strong ability to achieve robust sensor FTC. However, their application in electric drives or in grid connected converters still very limited [33-35].

The presented sensor fault estimation and compensation techniques applied to single-phase grid connected converters in [35] consider the use of grid voltage sensor. At the best known of the authors, sensor fault estimation techniques applied to grid sensorless SPGCC have not discussed yet by the literature. In this context, this paper proposes a robust and fast current sensor fault estimation and fault compensation method of an AC voltage sensorless controlled single phase grid connected converter. For this purpose, two PI observers are implemented. The first one aims to estimate accurately the grid voltage whereas the two other PI observers are intended to estimate the current sensor fault. The estimated fault is then used to reject the effects of the erroneous measurements through compensation technique.

The paper is organized as follows: First, in section 2, the converter model and its control strategy are presented. Section 3 is devoted to analyze the design of the PI based sensor fault estimation observer and the PI based grid voltage estimator is investigated in section 4. Simulation results are carried out in section 5. the experimental validation of the proposed sensorless current fault estimation and compensation algorithm is discussed in section 6. Finally, the paper is summed up in a conclusion in section 7.

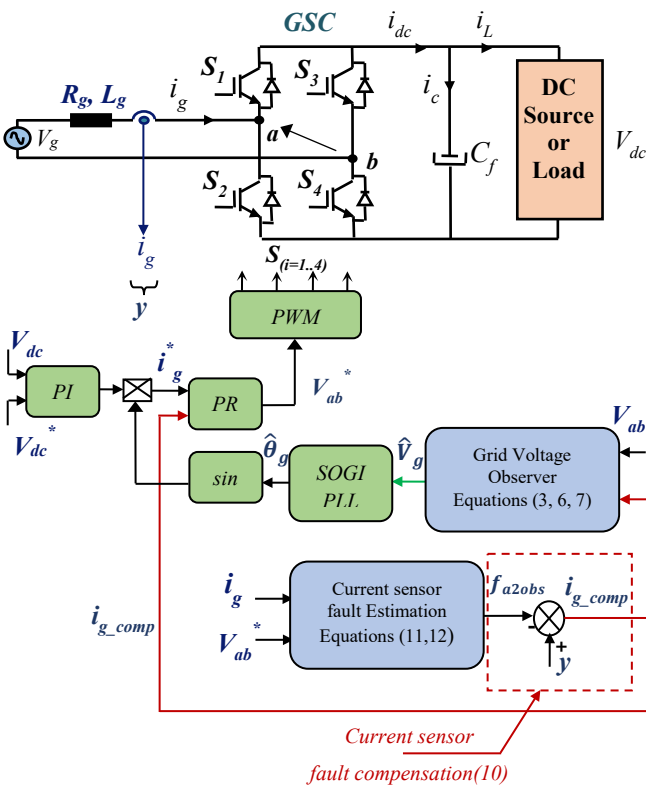
## 2. SPGCC Modelling

Fig.1 presents the main structure of the SPGCC and its control strategy. It includes also the grid voltage observer and the proposed sensor FTC strategy. The SPGCC consists of four IGBT-Diode switches ( $S_1$ - $S_4$ ) connected to a single phase AC voltage supply through series L filter and its internal resistance R. A DC capacitor  $C_f$  is connected to the DC voltage bus to maintain the voltage  $V_{dc}$  constant.

Supposing that the switches are ideal and neglecting the dead time, the system under study can be described as follows:

$$\begin{cases} V_g = R i_g + L \frac{di_g}{dt} + V_{ab} \\ i_c = i_{dc} + i_L = C \frac{dV_{dc}}{dt} \\ V_{ab} = (S_1 - S_3) V_{dc} \\ i_{dc} = (S_1 - S_3) i_g \end{cases} \quad (1)$$

Where  $V_g$ ,  $V_{ab}$ ,  $i_g$ ,  $i_{dc}$  and  $i_c$  are the grid voltage, the converter voltage, the grid current, the converter current and the capacitor current, respectively.



**Fig. 1.** Block diagram of the proposed grid voltage sensorless FTC system

The control loop of the SPGCC is a double closed loop. An external proportional-integral (PI) based control loop for DC-link voltage and an inner proportional-resonant (PR) based grid current control loop [36]. The current control loop of the SPGCC allows the grid current  $i_g$  to have a sinusoidal waveform and the inverter to work with a unity power factor. Hence, the generation of the grid current reference  $i_g^*$  requires accurate information of the grid phase angle  $\theta_g$  which is obtained through a second order generalized integrator (SOGI) phase locked-loop (PLL) module [37].

### 3. PI Observer Current Sensor Fault Estimation

#### 3.1. Observer Design

In this section, the design of the PI Observer dedicated to the current sensor fault reconstruction is detailed first. In this work we assume that all disturbances are rejected. Hence, the grid current state model with sensor faults is described by:

$$\begin{cases} \frac{di_g}{dt} = A i_g + B(V_g - V_{ab}) \\ y = i_g + F_i \end{cases} \quad (2)$$

Where  $A = -R/L$  and  $B = 1/L$ .  $F_i$  corresponds to the sensor fault and  $y$  is the output measurement vector.  $F_i$  is a bounded function, so,  $\|F_i\| \leq v_1$ , with  $v_1$  a positive known constant. By applying a first order linear filter to the output the system described by (2), a new variable  $x_1$  is defined as follows [34]:

$$\frac{dx_1}{dt} = -x_1 + y = -x_1 + i_g + F_i \quad (3)$$

Considering (2) and (3) a new system is expressed by equation (4)

$$\begin{cases} \frac{di_g}{dt} = \begin{bmatrix} A & 0 \\ 1 & -1 \end{bmatrix} \begin{bmatrix} i_g \\ x_1 \end{bmatrix} + \begin{bmatrix} B \\ 0 \end{bmatrix} (V_{ab} - V_g) + \begin{bmatrix} 0 \\ 1 \end{bmatrix} F_i \\ y_1 = \begin{bmatrix} 0 & 1 \end{bmatrix} \begin{bmatrix} i_g \\ x_1 \end{bmatrix} \end{cases} \quad (4)$$

Where  $y_1$  is the output of the system described by (4). It can be seen that  $F_i$  corresponds to an unknown input of that system. It is assumed that the amplitude, the time of occurrence as well the kind of the sensor fault are unknown. Consequently,  $F_i$  has to be estimated using the PI observer. PI observers are a kind of extended state observers that use both proportional and integrating actions. They are useful for system's disturbances and unknown inputs estimation [38]. Accordingly, in this work, two PI observers are designed and are applied to state systems of (2) and (4) in order to estimate the grid voltage and the current sensor fault respectively.

In order to guarantee the current sensor fault reconstruction for the grid voltage sensorless controlled SPGCC, it is necessary that the system defined in (4) is decoupled from grid voltage estimated value. Hence some modifications should be introduced on system (4):

$$\begin{cases} \frac{di_g}{dt} = (A + \Delta A) i_g + (B + \Delta B) V_{ab} + (B + \Delta B) V_g \\ \frac{di_g}{dt} = A i_g + B V_{ab} + \Delta A i_g + \Delta B V_{ab} + (B + \Delta B) V_g \\ \frac{di_g}{dt} = A i_g + B V_{ab} + D d \end{cases} \quad (5)$$

Where  $\Delta A = \Delta R / \Delta L$ ,  $\Delta B = 1 / \Delta L$ ,  $D = 1$  and  $d = \Delta i_g + \Delta B V_{ab} + (B + \Delta B) V_{ab}$ . Here  $d$  includes the disturbances introduced by system's parameters mismatches and grid voltage sensorless.

Finally, the state system of (4) is decoupled from the grid voltage and it can be rewritten as:

$$\begin{cases} \frac{di_g}{dt} \\ \frac{dx_1}{dt} \end{cases} = \begin{bmatrix} A & 0 \\ 1 & -1 \end{bmatrix} \begin{bmatrix} i_g \\ x_1 \end{bmatrix} + \begin{bmatrix} B \\ 0 \end{bmatrix} V_{ab} + \begin{bmatrix} 0 \\ 1 \end{bmatrix} F_i + \begin{bmatrix} 1 \\ 0 \end{bmatrix} d \quad (6)$$

$$y_1 = \begin{bmatrix} 0 & 1 \end{bmatrix} \begin{bmatrix} i_g \\ x_1 \end{bmatrix}$$

The structure of the proposed PI observer is presented in Fig. 2.

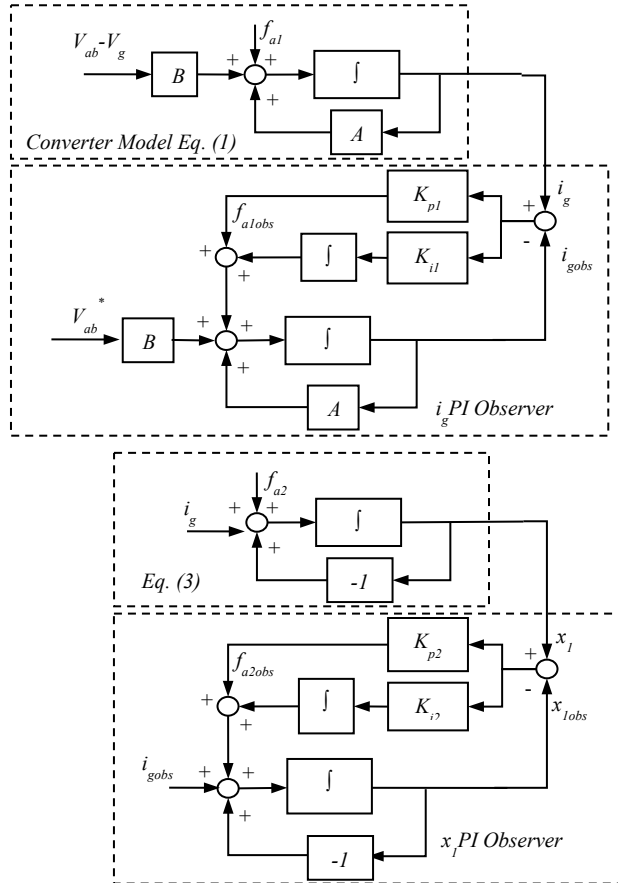


**Fig. 2.** Structure of the PI-based current fault estimation observer

The dynamics of the PI-observers is expressed as:

$$\begin{cases} \frac{di_{gobs}}{dt} \\ \frac{df_{a1obs}}{dt} \end{cases} = \begin{bmatrix} A & 1 \\ 0 & 0 \end{bmatrix} \begin{bmatrix} i_{gobs} \\ f_{a1obs} \end{bmatrix} + \begin{bmatrix} B \\ 0 \end{bmatrix} (V_{ab}^* - V_{gobs}) + \begin{bmatrix} K_{p1} \\ K_{i1} \end{bmatrix} (i_g - i_{gobs}) \quad (7)$$

$$\begin{cases} \frac{dx_{1obs}}{dt} \\ \frac{df_{a2obs}}{dt} \end{cases} = \begin{bmatrix} -1 & 1 \\ 0 & 0 \end{bmatrix} \begin{bmatrix} x_{1obs} \\ f_{a2obs} \end{bmatrix} + \begin{bmatrix} 1 \\ 0 \end{bmatrix} i_{gobs} + \begin{bmatrix} K_{p2} \\ K_{i2} \end{bmatrix} (x_1 - x_{1obs})$$

Where  $K_{p1}$ ,  $K_{i1}$ ,  $K_{p2}$  and  $K_{i2}$  are successively the proportional and integral gains of each observer. Moreover,  $f_{a1obs}$  and  $f_{a2obs}$  correspond to the estimated values of the disturbances and the sensor fault  $d$  and  $F_i$  respectively. They are defined as the integral of the difference  $(i_g - i_{gobs})$  and  $(x_1 - x_{1obs})$ .

### 3.2. Observer Stability Analysis

Consider the estimation errors as:  $e_i = i_g - i_{gobs}$ ,  $e_{x1} = x_1 - x_{1obs}$ ,  $e_{fa1} = f_{a1} - f_{a1obs}$ ,  $e_{fa2} = f_{a2} - f_{a2obs}$ , the error dynamics of (6):

$$\begin{cases} \frac{de_i}{dt} \\ \frac{de_{fa1}}{dt} \end{cases} = \frac{d}{dt} \begin{bmatrix} e_i \\ e_{fa1} \end{bmatrix} = \begin{bmatrix} A - K_{p1} & 1 \\ -K_{i1} & 0 \end{bmatrix} \begin{bmatrix} e_i \\ e_{fa1} \end{bmatrix} - \begin{bmatrix} 0 \\ f_{a1} \end{bmatrix} \quad (8)$$

$$\begin{cases} \frac{de_{x1}}{dt} \\ \frac{de_{fa2}}{dt} \end{cases} = \frac{d}{dt} \begin{bmatrix} e_{x1} \\ e_{fa2} \end{bmatrix} = \begin{bmatrix} -1 - K_{p2} & 1 \\ -K_{i2} & 0 \end{bmatrix} \begin{bmatrix} e_{x1} \\ e_{fa2} \end{bmatrix} - \begin{bmatrix} 0 \\ f_{a2} \end{bmatrix}$$

The parameters  $K_{p1}$ ,  $K_{i1}$ ,  $K_{p2}$  and  $K_{i2}$  are selected in order to guarantee the convergence of all estimation errors to zero which allows the estimation states to converge to the actual states. The observers' gains values are selected using pole placement method. The poles of the observers characteristic polynomials, expressed in (9), have negative real parts:

$$\begin{cases} F_1(s) = s^2 + \left(\frac{R}{L} + K_{p1}\right)s + K_{i1} \\ F_2(s) = s^2 + (1 + K_{p2})s + K_{i2} \end{cases} \quad (9)$$

### 3.3. Sensor fault Tolerance process

Once the sensor fault estimation is achieved, the sensor fault tolerance is triggered by sensor fault effects rejection [34] as follows:

$$i_{g\_comp} = y - F_{iobs} \quad (10)$$

Where  $i_{g\_comp}$  is the compensated output. As presented in Fig. 1, the current sensor FTC process is integrated into controller structure. Consequently, in order to ensure high performances of the inverter with accurate grid voltage estimation during post-fault operation, the original output  $y$  is replaced by the compensated one  $i_{g\_comp}$  as the input to the current control loop as well as the input to the grid voltage PI-observer block.

## 4. PI Observer Grid Voltage Estimation

According to the definition of the PI-observer and following the same analysis as in the previous section, it is clear that the grid voltage may be estimated using a PI-observer when it is treated as an unknown input of the system in (1). Accordingly, the structure of the grid voltage PI observer, with the consideration of the proposed sensor FTC, is given by:

$$\frac{d}{dt} \begin{bmatrix} i_{gobs-comp} \\ f_{a3obs} \end{bmatrix} = \begin{bmatrix} A & 1 \\ 0 & 0 \end{bmatrix} \begin{bmatrix} i_{gobs-comp} \\ f_{a3obs} \end{bmatrix} + \begin{bmatrix} B \\ 0 \end{bmatrix} V_{ab}^* + \begin{bmatrix} K_{p3} \\ K_{i3} \end{bmatrix} (i_{g-comp} - i_{gobs-comp}) \quad (11)$$

Where  $f_{a3obs} = \int (i_{g-comp} - i_{gobs-comp}) dt$ . According to (1) and (11), since the grid voltage is estimated by the PI observer,  $f_{a3obs}$  is described by:

$$f_{a3obs} = \frac{-V_{gobs}}{L} \quad (12)$$

From equation (11) we can see that the dynamics of the PI-observer based  $V_g$  estimator is the same of the PI-observer presented in (6). Hence, with appropriate choice of  $K_{p3}$  and  $K_{i3}$  using pole placement technique, we can guarantee that  $V_{gobs}$  will converge to its real state  $V_g$ .

### 5. Simulation Results

In order to verify the performances of the proposed grid voltage sensorless control and the grid current sensor fault estimation and compensation, simulation tests were first carried out under Matlab-Simulink environment tool. The main system parameters used for simulation are carried out in Table I.

In all tests, the measured grid voltage is not used for the control loop but only displayed for comparison.

Two kinds of faults are investigated:

$$\begin{cases} i_g(t) = I \sin(\omega_g t): \text{ Healthy sensor operation} \\ i_g(t) = I \sin(\omega_g t) + K, K \in \mathfrak{R}: \text{ DC offset sensor fault} \\ i_g(t) = a I \sin(\omega_g t), a \in \mathfrak{R}: \text{ Gain sensor fault} \end{cases}$$

**Table 1.**Parameter Values for simulation

Converter's Parameters	
Grid voltage $V_{gRMS}$	48V
Line resistance $R_g$	$0.2\Omega$
Line inductance $L_g$	0.87mH
dc-link voltage $V_{dc}$	80V
dc-link capacitor C	1100uF
Grid frequency f	50 Hz
Maximum variable Load resistance $R_L$	$54\Omega$
Load inductance L	1mH
Sample time $T_s$	100 us
PI-based Current Sensor Fault Observer's Parameters	
$K_{p1}$	$1e^6$
$K_{i1}$	$1.9e^5$
$K_{p2}$	$1e^5$
$K_{i2}$	0.5
PI-based grid Voltage Observer's Parameters	
$K_{p3}$	200
$K_{i3}$	$1e^5$

Using these conditions, four different cases are discussed:

**Case 1:** The simulation results of the first sensor fault case is shown in Fig4. Initially, the system runs in healthy operation mode without knowledge of the grid voltage. It can be noted from Fig4.c that the GPI observer estimates with good accuracy and good dynamic the grid voltage, hence the SPGCC can effectively achieve grid synchronization. In the same time, during healthy operation mode ( $t \leq 0.8s$ ) (Fig4.a), the estimated grid current sensor fault remain at a very low level and the compensated current  $i_{gcomp}$  coincides with the measured one  $i_g$  (Fig4.b). As presented in Fig4.a, at  $t=0.8s$ , a 80% dc-

offset current sensor fault occurs. Immediately,  $F_{iobs}$  starts to reach its actual current sensor fault value  $F_i$ . In addition, it is clearly that the compensated current maintains good performances. Similarly, the grid voltage observer maintains its good performances and the estimated grid voltage keeps following the actual voltage with an accurate estimation of the grid phase angle  $\theta_{gobs}$  and the unity power factor operation of the converter is maintained. At  $t=1.2s$ , a 50% variation of DC load is applied causing a step jump of the DC current from 1.5A to 3A. It can be observed that the proposed FE-FTC keeps its good performances. In conclusion, the sensor is well isolated and the converter's performances are not degraded.

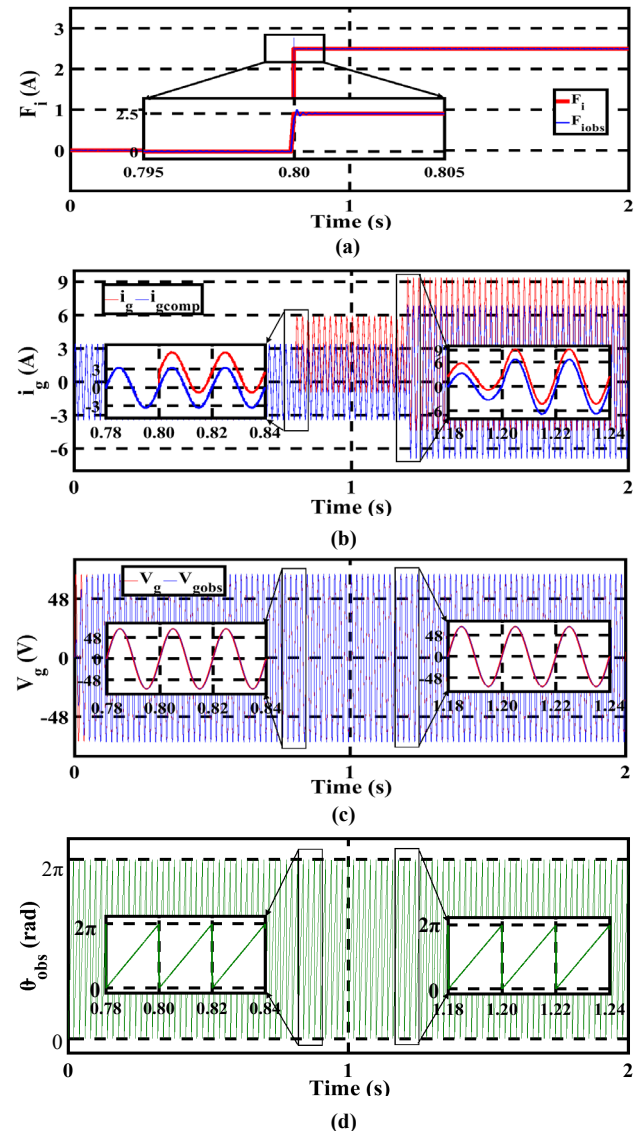


**Fig. 4.** Simulation results of case 1 under dc-load variation: (a) actual and estimated current sensor fault  $F_i$ ,  $F_{iobs}$  (b) Measured current  $i_g$  and compensated output  $i_{gcomp}$  (c) Actual grid voltage  $V_g$ , observed grid voltage  $V_{gobs}$  (d) observed phase angle  $\theta_{gobs}$

**Case 2:** In this case, the ability of the proposed FTC approach under current sensor gain fault is discussed. As

depicted out in Fig. 5a, at time  $t=0.8s$ , a 80% gain fault is introduced. As in case 1,  $F_{iobs}$  coincides with the actual current fault. In addition, the transient system performance in presence of the current sensor fault is depicted in Fig5.b-c-d. It is shown that the current sensor fault is immediately isolated. The compensated current  $i_{gcomp}$  is then introduced into the control loop ensuring a unity power operation. Similarly to the other fault scenarios, a 50% variation of the dc load was introduced at  $t=1.2s$  resulting in the variation of the dc-current from 1.5A to 3 A. It can be seen that the proposed sensorless fault estimation and compensation method is proven to be very fast and efficient

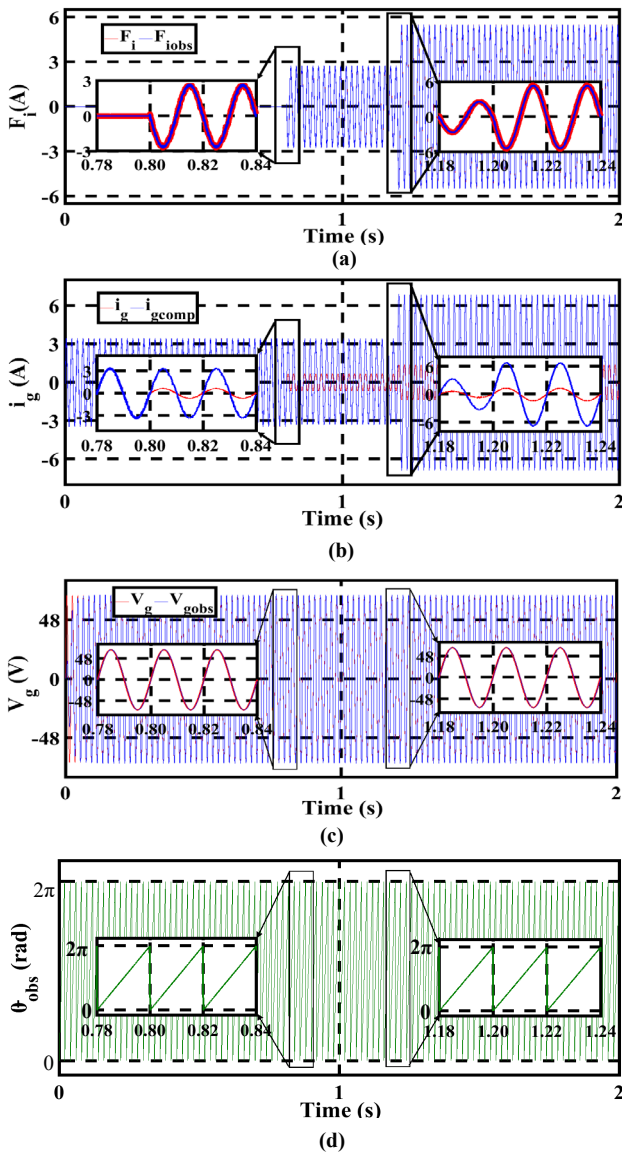


**Fig. 5.** Simulation results of case 2 dc-load variation: (a) actual and estimated current sensor fault  $F_i, F_{iobs}$  (b) Measured current  $i_g$  and compensated output  $i_{gcomp}$  (c) Actual grid voltage  $V_g$ , observed grid voltage  $V_{gobs}$  (d) observed phase angle  $\theta_{gobs}$

**Case 3:** Fig6 presents the grid voltage sensorless startup process in presence of a 80% dc-offset current fault: The converter’s controller is activated at time  $t = 0.5s$ . As

depicted out in Fig6.a, the estimated current sensor fault  $F_{iobs}$  tracks precisely its actual value  $F_i$  with an almost zero estimation error. In addition, Fig6.b-c-d illustrate respectively the actual and compensated grid current, the actual and estimated grid voltage and the estimated grid angle. As can be seen, it takes only 20ms for the estimated grid voltage to reach the actual voltage value. Moreover, the compensated grid current presents a highly sinusoidal waveform with a unity power factor operation confirming the effectiveness of the proposed sensorless fault estimation and compensation control technique. In summary, it can be concluded that converter keeps its good performances by presenting a sinusoidal grid current with low harmonic distortion and the grid power factor is equal to 1.

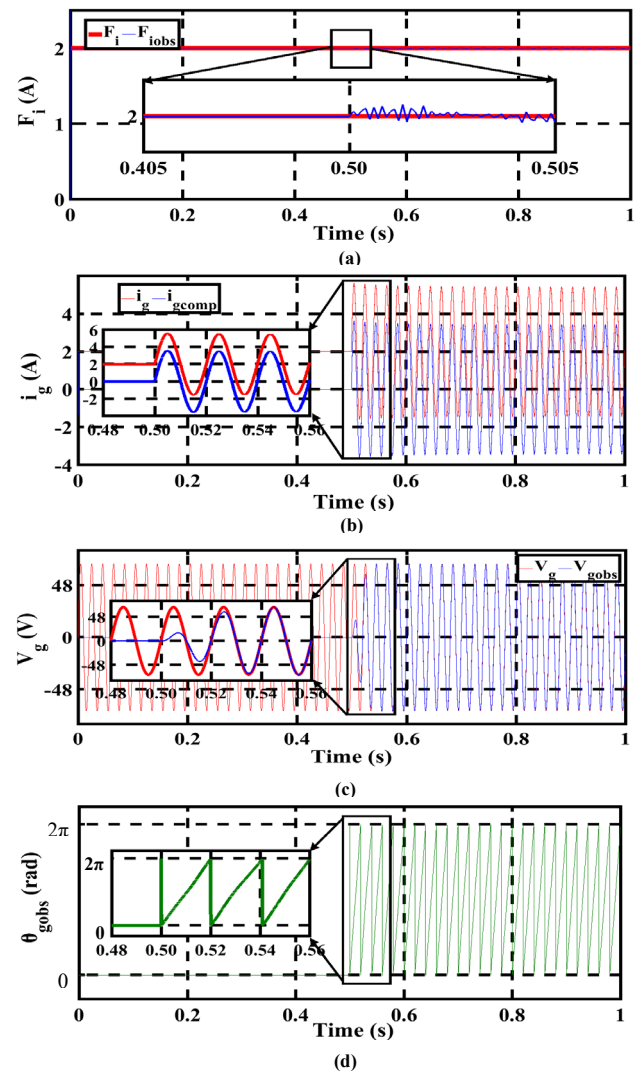


**Fig. 6.** Simulation results of case 3: (a) actual and estimated current sensor fault  $F_i, F_{iobs}$  (b) Measured current  $i_g$  and compensated output  $i_{gcomp}$  (c) Actual grid voltage  $V_g$ , observed grid voltage  $V_{gobs}$  (d) observed phase angle  $\theta_{gobs}$

**Case 4:** Similarly to case 3, the converter’s controller is activated at time  $t = 0.5s$ , when the current sensor is already under a 80% gain fault. As shown in Fig.7, the

obtained results illustrated the effectiveness of the proposed approach during the startup of the converter.

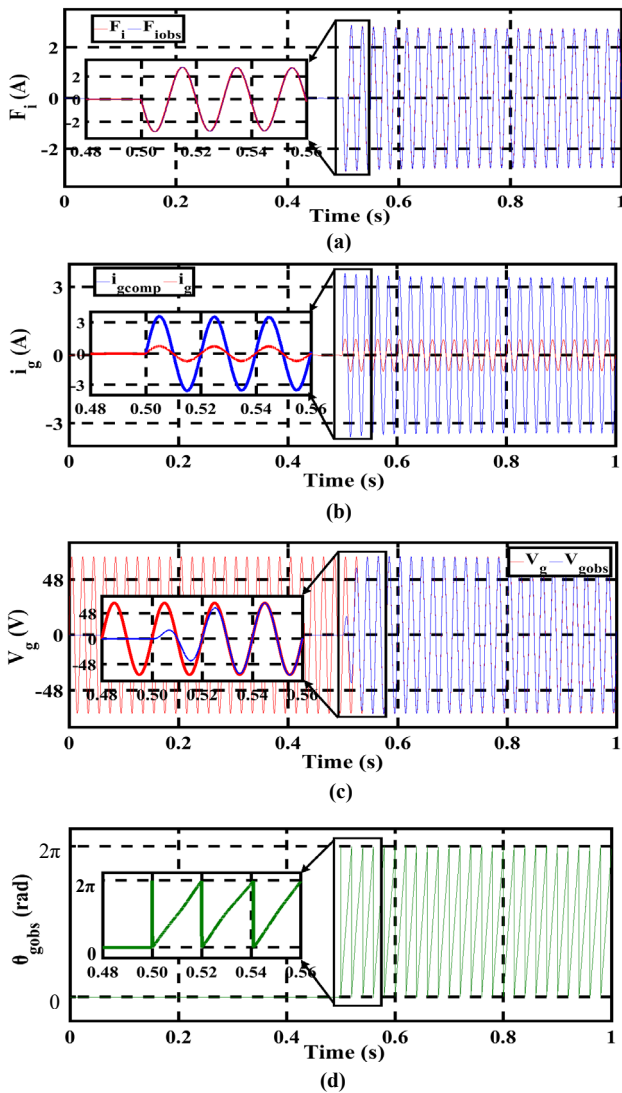


**Fig. 7.** Simulation results of case 4: (a) actual and estimated current sensor fault  $F_i$ ,  $F_{iobs}$  (b) Measured current  $i_g$  and compensated output  $i_{g\_comp}$  (c) Actual grid voltage  $V_g$ , observed grid voltage  $V_{gobs}$  (d) observed phase angle  $\theta_{gobs}$

**6. Experimental Results**

**6.1. Experimental setup description**

The effectiveness and the feasibility of the proposed sensor FTC approach of the grid voltage sensorless controlled SPGCC are experimentally verified. The structure of the experimental setup is presented in Fig8. It comprises basically one Semikron SKiiP voltage source converter used as a single PWM inverter, with a DC bus capacitor bank of 1100 $\mu$ F. The DC-link voltage is fixed at  $V_{dc} = 80V$ . The inverter is connected to the main grid through an  $L$  filter ( $L = 20mH, R = 0.2\Omega$ ) and a 230V/48V transformer. The grid current measurement is ensured by a LEM PR 30 current sensor. The proposed control, grid voltage estimation and FE-based FTC algorithms are

implemented on a dSPACE DS1104 digital controller. The sampling time  $T_s = 100\mu s$  and the PWM frequency set to 10 kHz. All the results are captured using dSPACE DS1104 digital controller and then plotted using Keithley USB data-acquisition module.

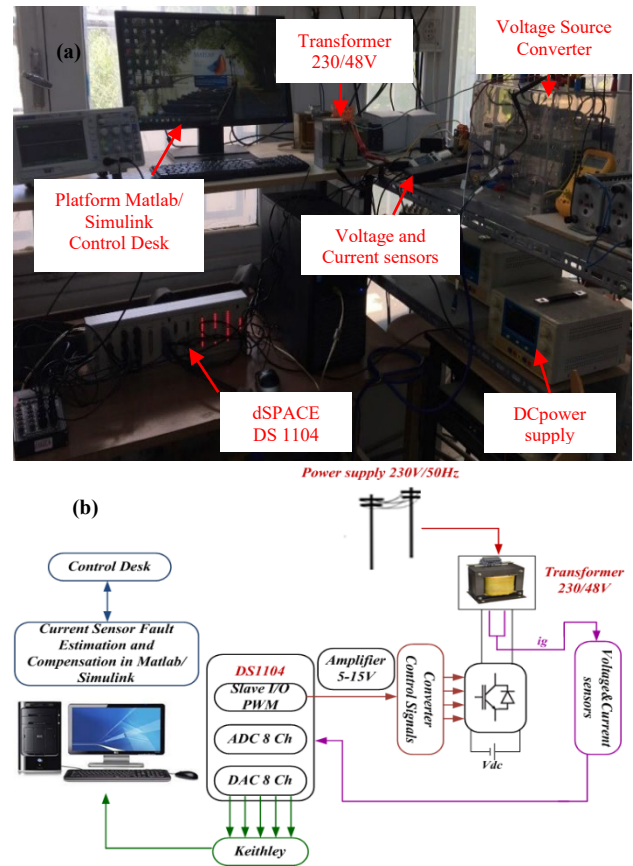


**Fig. 8.** Experimental implementation (a) experimental test bench (b) description diagram of the experimental implementation

The different PI observers parameters used for experimental implementation are carried out in Table II.

**Table 2.**Parameter Values for experimental implementation

PI-based Current Sensor Fault Observer's Parameters	
$K_{p1}$	$1e^4$
$K_{i1}$	$1e^3$
$K_{p2}$	90
$K_{i2}$	0.5
PI-based grid Voltage Observer's Parameters	
$K_{p3}$	100
$K_{i3}$	$1e^5$

The same cases are chosen for experimental implementation tests as in the simulation.

**6.2. Proposed FE-FTC performances analysis**

**Case 1:** The experimental results of the 80% dc-offset grid current fault are depicted in Fig.9. It can be seen that with no initial knowledge of the grid voltage, a stable start-up is ensured. Specifically, Fig.9.c shows that estimated and the actual grid voltage are superimposed. At  $t=1.60$ , a 80% offset fault of the grid current sensor is introduced.

Consequently, and according to Fig9.a, the estimated sensor fault tracks accurately the actual sensor fault with an estimation error of 0.2A. Moreover, the estimated voltage  $V_{gobs}$  is highly in consistency with the actual measured grid voltage and an accurate estimation of the grid phase angle  $\theta_{gobs}$  is ensured in both healthy and post-fault operation modes. While, the measured current is severely affected by the injected fault, the compensated current  $i_{gcomp}$  maintains good performance. Finally, the performances of the inverter during post-fault operation are the same as in healthy operation mode, where the compensated output  $i_{gcomp}$  is in phase with the actual grid voltage  $V_g$ .

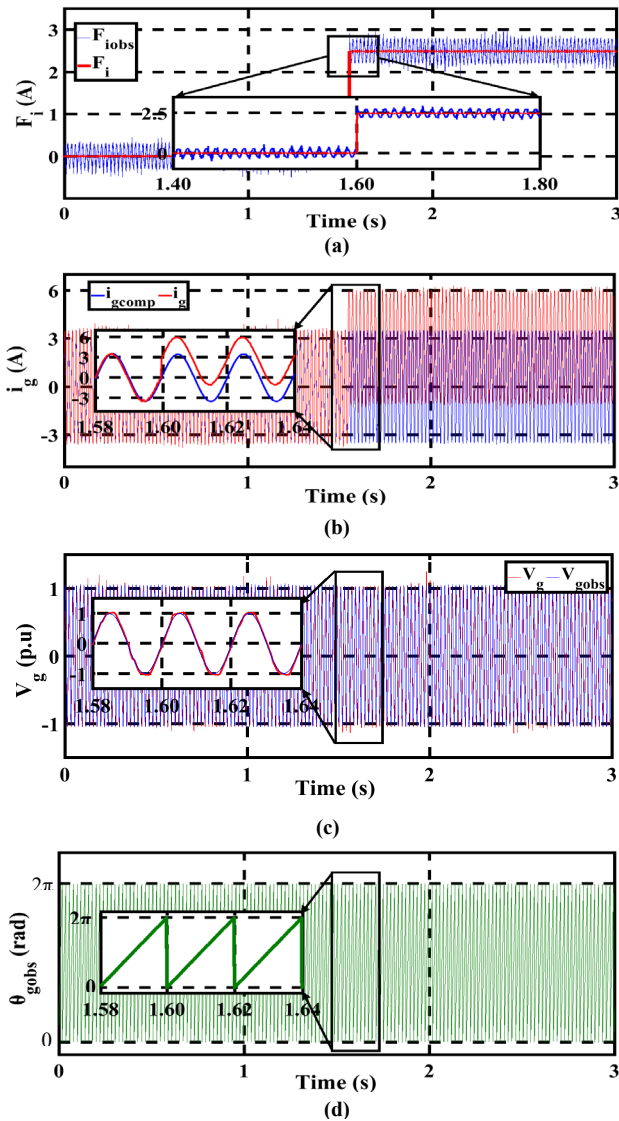


**Fig. 9.** Experimental results of case 1 : (a) actual and estimated current sensor fault  $F_i$ ,  $F_{iobs}$  (b) Measured current  $i_g$  and compensated output  $i_{g\_comp}$  (c) Actual grid voltage  $V_g$ , observed grid voltage  $V_{gobs}$  (d) observed phase angle  $\theta_{gobs}$

**Case 2:** Fig.10 shows the experimental results for compensation of a 80% gain fault of the grid current sensor. As shown in the figure, a stable startup is ensured

by the proposed grid voltage sensorless algorithm. At  $t=1.40$ s, a 80% current sensor gain fault is introduced. Consequently, the current fault signal  $F_i$  switches from zero to  $\pm 2.8$ A and the estimated sensor fault  $F_{iobs}$  tracks precisely the actual sensor fault  $F_i$ . Moreover, it can be observed from Fig10.b that the estimated grid voltage  $V_{gobs}$  tracks the measured voltage without any noticeable dynamics in the waveform during post-fault operation. Consequently, the effectiveness of the proposed approach in both healthy and faulty mode operation modes is once again ensured.

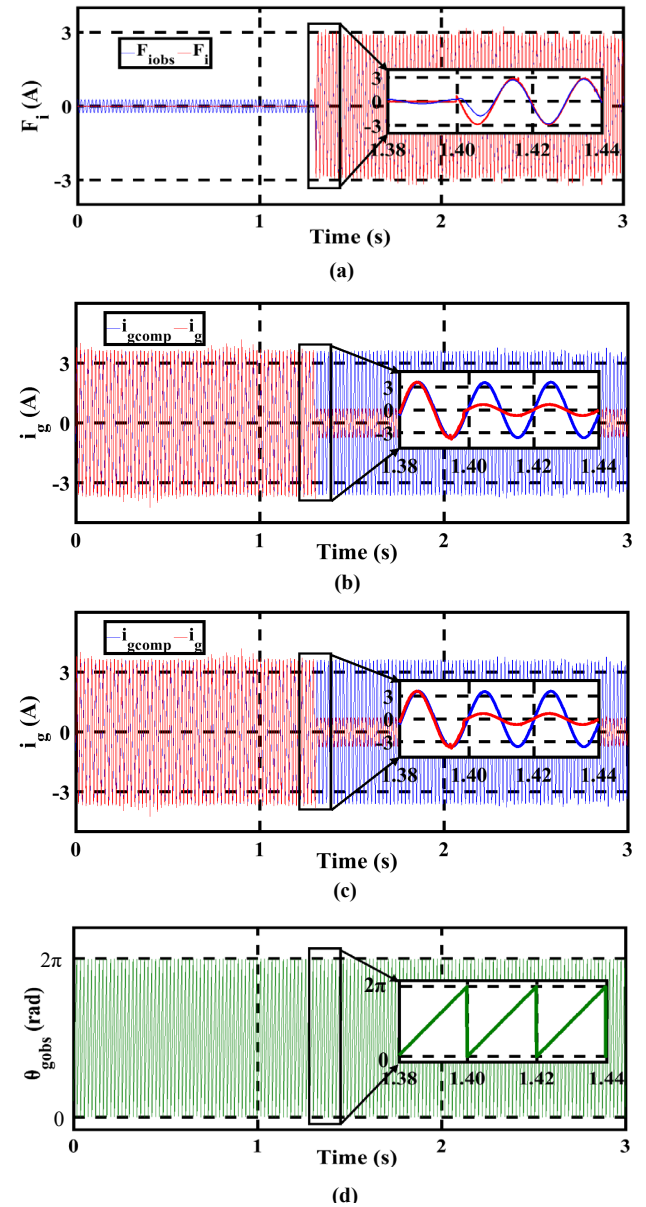


**Fig. 10.** Experimental results of case 2 : (a) actual and estimated current sensor fault  $F_i$ ,  $F_{iobs}$  (b) Measured current  $i_g$  and compensated output  $i_{g\_comp}$  (c) Actual grid voltage  $V_g$ , observed grid voltage  $V_{gobs}$  (d) observed phase angle  $\theta_{gobs}$

**Case 3:** In Fig11 is presented the experimental results of the grid voltage sensorless converter's startup under a 80% dc-offset fault of the grid current sensor. It can be seen

from Fig11.a that the estimated current fault  $F_{iobs}$  tracks accurately the actual fault with an estimation error of 0.08A. As for the estimation of the grid voltage, it is clear that the estimated voltage efficiently tracks the measured grid voltage after only 12ms. Moreover, the current fault was immediately rejected and the compensated grid current keeps a perfectly sinusoidal shape in phase with the grid voltage. In summary, the proposed grid voltage sensorless control and the grid current sensor fault estimation and compensation is very fast and efficient.

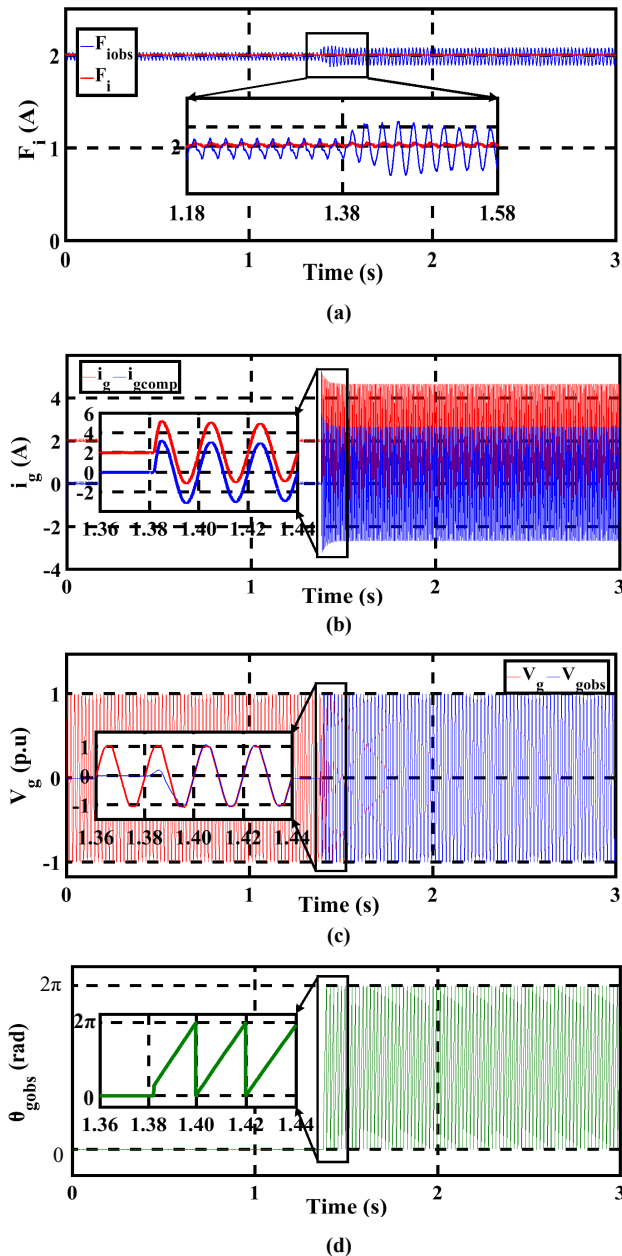


**Fig. 11.** Experimental results of case 3 : (a) actual and estimated current sensor fault  $F_i$ ,  $F_{iobs}$  (b) Measured current  $i_g$  and compensated output  $i_{g\_comp}$  (c) Actual grid voltage  $V_g$ , observed grid voltage  $V_{gobs}$  (d) observed phase angle  $\theta_{gobs}$

**Case 4:** A second test for the grid voltage sensorless start up of the converter closed loop operation under 80% gain

fault of the grid current sensor was performed (Fig12). It can be seen in Fig12.a that before the activation of converter's control, the estimated current fault remain at a very low level almost at zero. Hence, once the converter's controller is activated at  $t=1.88$ s, the estimated current fault starts to track precisely the actual fault. Fig12. b-c-d illustrate respectively the estimated grid angle, the measured and estimated grid voltage and the faulty and compensated grid current. As can be seen from Fig12.c, the estimated grid voltage  $V_{gobs}$  reaches its actual value with an accurate estimation of the grid angle. Furthermore and as described by Fig12.b, the compensated output  $i_{g\_comp}$  keeps good performances with a sinusoidal shape and a unity power factor.

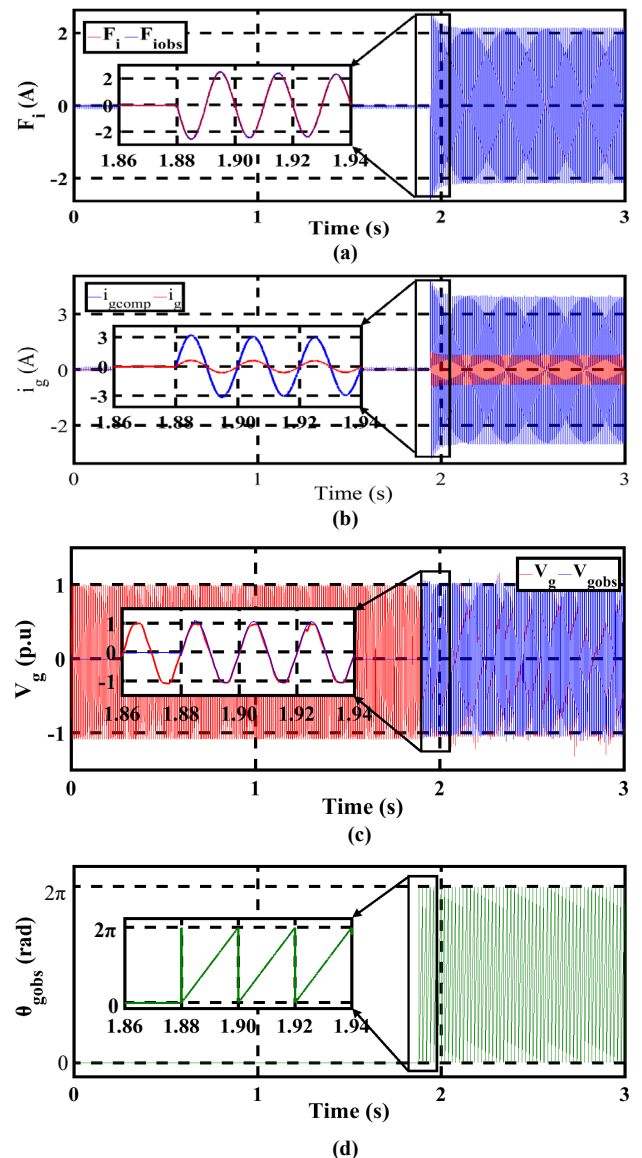


**Fig. 12.** Experimental results of case 4 : (a) actual and estimated current sensor fault  $F_i$ ,  $F_{iobs}$  (b) Measured current  $i_g$  and compensated output  $i_{g\_comp}$  (c) Actual grid voltage  $V_g$ , observed grid voltage  $V_{gobs}$  (d) observed phase angle  $\theta_{gobs}$

### 6.3. Proposed FE-FTC scheme vs conventional FDI-FTC methods

The proposed FE-FTC scheme is compared with classical FDI-FTC approaches. The obtained results show that the performances of the grid connected converter during sensor post-fault operation are similar to those obtained under healthy operation conditions: sinusoidal waveform of the grid current with unity power factor operation in the grid side. Moreover, the grid voltage is well estimated. It can be seen also that the sensor fault estimation and compensation is achieved without any appreciable delay. This leads to a slight transient during control reconfiguration. As mentioned above, the proposed FTC does not need any fault detection threshold, which increase its robustness and offers more flexibility for its real time implementation compared to classical FDI-FTC approaches. The proposed FE-FTC approach is a model based one. Hence, it is dependent of the systems' parameters. The observer should be carefully designed in order to reduce, as much as possible, the impact of the systems' parameters mismatch on the FE-FTC algorithm performances. In this work, only sensor faults have been considered. However, the state of the art review demonstrates that in addition to modeling uncertainties, disturbances affect the quality and robustness of the FTC system [35-37]. Hence, to guarantee robust FE-FTC system, it is necessary to decouple disturbances from sensor faults, which will be discussed in future work.

## 7. Conclusion

In this paper, fast and effective fault estimation based current sensor fault tolerant control of a grid voltage sensorless controlled SPGCC is presented. The grid voltage estimation as well the current sensor fault reconstruction have been realized through a bank of proportional-integral observers. The sensor FTC algorithm consists on sensor fault compensation. Both simulation and experimental results considering dc offset and gain faults of the grid current sensor have been presented. They show the accurate reconstruction of the sensor faults. In the same time, the system is not affected by the sensor fault and maintains high performances during post-fault operation in terms of grid current sinusoidal absorption, high power factor operation with good estimation of the grid voltage. Compared to classical FDI-FTC techniques, the proposed FTC scheme offers more flexibility and ability of achieve robust sensor FTC of grid connected converters.

## References

- [1] Y. Yang & F. Blaabjerg (2015) Overview of single-phase Grid Connected Photovoltaic Systems, *Electric Power Components and Systems*, 43:12, 1352-1363
- [2] T. T. GUINGANE, D. BONKOUNGOU, E. KORSAGA, E. SIMONGUY, Z. KOALAGA and F. ZOUGMORE, "Modeling and Simulation of a Photovoltaic System Connected to The Electricity Grid with MATLAB/Simulink/ Simpower Software," 2020 8th International Conference on Smart Grid (icSmartGrid), 2020, pp. 163-168,
- [3] S. SALAH, E. CHARQAOUY, D. SAIFAOU, O. BENZOHRRA, A. LEBSIR (2020), Integration of Decentralized Generations into the Distribution Network- Smart Grid Downstream of the Meter, *International Journal of Smart Grid (ijSmartGrid)*, ISSN: 2602-439X, Vol 4, No 1, pp.18-27
- [4] C. Khomsi, M. Bouzid, K. Jelassi. Power Quality Improvement in a Three-Phase Grid Tied Photovoltaic System Supplying Unbalanced and Nonlinear Loads. *Int. J. Renew. Energy Res.* 2018, 8, 1165–1177.
- [5] A. B. Youssef, S. Khojet El Khil and I. S. Belkhdja, "State Observer-Based Sensor Fault Detection and Isolation, and Fault Tolerant Control of a Single-Phase PWM Rectifier for Electric Railway Traction," in *IEEE Trans on Power Electronics*, vol. 28, no. 12, pp. 5842-5853, Dec. 2013.
- [6] L. Schirone and M. Macellari, "A techno-economical analysis of charge management in electrical vehicles," 2015 Int. Conf. Renew. Energy Res. Appl. ICRERA 2015, pp. 1253–1258, 2016.
- [7] T. Sakagami, Y. Shimizu and H. Kitano, "Exchangeable batteries for micro EVs and renewable energy," 2017 IEEE 6th International Conference on Renewable Energy Research and Applications (ICRERA), 2017, pp. 701-705
- [8] H. Yang, Y. Zhang, J. Liang, J. Gao, P. D. Walker and N. Zhang, "Sliding-Mode Observer Based Voltage-Sensorless Model Predictive Power Control of PWM Rectifier Under Unbalanced Grid Conditions," in *IEEE Transactions on Industrial Electronics*, vol. 65, no. 7, pp. 5550-5560, July 2018.
- [9] G. Leilei & Li. Yanyan & Jin, Nan & Dou, Zhifeng & Wu, Jie. (2020). Sliding Mode Observer Based AC Voltage Sensorless Model Predictive Control for Grid-Connected Inverters. *IET Power Electronics*.
- [10] A. B. Youssef, S. Khojet El Khil and I. S. Belkhdja. (2017). Open-circuit fault diagnosis and voltage sensor fault tolerant control of a single phase pulsed width modulated rectifier. *Mathematics and Computers in Simulation*, 131, 234-252.
- [11] A. Rahoui, A. Bechouche, H. Seddiki, & D. Abdeslam, (2020). Virtual flux estimation for sensorless predictive control of pwm rectifiers under unbalanced and distorted grid conditions. *IEEE Journal of Emerging and Selected Topics in Power Electronics*, 9(2), 1923-1937.
- [12] J. Liang, H. Wang, H & Z. Yan, (2019). Grid voltage sensorless model-based predictive power control of PWM rectifiers based on sliding mode virtual flux observer. *IEEE Access*, 7, 24007-24016.
- [13] S. Bayhan. (2021). Grid Voltage Sensorless Model Predictive Control for a Single-Phase T-Type Rectifier With an Active Power Decoupling Circuit. *IEEE Access*, 9, 19161-19174.
- [14] M. Mehreganfar & S. Davari, (2017, September). Sensorless predictive control method of three-phase AFE rectifier with MRAS observer for robust control. In *2017 IEEE International Symposium on*

- Predictive Control of Electrical Drives and Power Electronics (PRECEDE)* (pp. 107-112). IEEE.
- [15] M. Dardouri, S. K. El Khil and K. Jelassi, "Sensorless Active Damping of LCL\_Filter based on MRAS Estimator for Single-Phase Grid-Connected Inverter," 2019 10th International Renewable Energy Congress (IREC), Sousse, Tunisia, 2019, pp. 1-5.
- [16] N.B. Lai, K.H. Kim & P. Rodriguez, (2019). Voltage sensorless control scheme based on extended-state estimator for a grid-connected inverter. *IEEE Transactions on Power Electronics*, 35(6), 5873-5882
- [17] G. Zhiwei, C. Cecati and S.X. Ding, "A survey of fault diagnosis and fault-tolerant techniques\_Part I: Fault Diagnosis with model-based and signal-based approaches", IEEE Trans. Ind. Electron., vol. 62, no. 6, pp. 3757–3767, Mar. 2015.
- [18] G. Zhiwei, C. Cecati and S.X. Ding, "A survey of fault diagnosis and fault-tolerant techniques\_Part II: Fault Diagnosis with knowledge-based and hybrid/active approaches", IEEE Trans. Ind. Electron., vol. 62, no. 6, pp. 3768–3774, Apr. 2015.
- [19] A. B. Youssef, S. Khojet El Khil and I. S. Belkhdja. (2018). "Single Phase PWM Rectifier Sensor Fault Tolerant Control Based on Residual Generation", *Journal of Electrical Systems*, 14 - 4, 2018. *Journal of Electrical Systems*. 14. 190 - 20'.
- [20] M. Tiar, A. Betka, S. Drid, S. Abdeddaim, M. Sellali, & S. Medjmadj, (2019). "Fault-tolerant control of a smart PV-grid hybrid system", *IET Renewable Power Generation*, 13(13), 2451-2461.
- [21] Jinhui Xia, Student Member, IEEE, YuanboGuo, Member,IEEE, Bijun Dai, and Xiaohua Zhang, « *Sensor Fault Diagnosis and System Reconfiguration Approach for an Electric Traction PWM Rectifier Based on Sliding Mode Observer*», IEEE Trans. Ind. Electron, vol. 532, no. 5, Sep-Oct2017.
- [22] F. Ben Youssef, L. Sbita, *Sensors fault diagnosis and fault tolerant control for grid connected PV system*, *International Journal of Hydrogen Energy* (2016)
- [23] C. Wu, C. Guo, Z. Xie, F. Ni, and H. Liu, "A Signal-Based Fault Detection and Tolerance Control Method of Current Sensor for PMSM Drive", IEEE Trans. Ind. Electron.
- [24] M. Merai, M. W. Naouar, I. Slama-Belkhdja, and E. Monmasson, "FPGA-Based Fault Tolerant Space Vector Hysteresis Current Control for Three-Phase Grid Connected Converter", IEEE Trans. Ind. Electron., vol. PP, no. 99, 2016.
- [25] S. Khojet El Khil, I. Jlassi, A. J. Marques Cardoso, J. O. Estima and N. Mrabet-Bellaaj, "Diagnosis of Open-Switch and Current Sensor Faults in PMSM Drives Through Stator Current Analysis," in IEEE Transactions on Industry Applications, vol. 55, no. 6, pp. 5925-5937, Nov.-Dec. 2019.
- [26] S. Karimi, A. Gaillard, P. Poure, and S. Saadate, "Current sensor fault tolerant control for WECS with DFIG," IEEE Trans. Ind. Electron., vol. 56, no. 11, pp. 4660–4670, Nov. 2009.
- [27] Y. Xia, Y. Xu & B. Gou. (2021). Current sensor fault diagnosis and fault-tolerant control for single-phase PWM rectifier based on a hybrid model-based and data-driven method. *IET Power Electronics*, 13(18), 4150-4157.
- [28] S. U. Jan, Y. D. Lee, J. Shin, and I. Koo, "Sensor fault classification based on support vector machine and statistical time-domain features," IEEE Access, vol.5, pp. 8682–8690, Jun. 2017.
- [29] B. Gou, Y. Xu, Y. Xia, G. Wilson, and S. Liu, "An intelligent time adaptive data-driven method for sensor fault diagnosis in induction motor drive system," IEEE Trans. Ind. Electron.
- [30] N. M. B. Lakhali, L. Adouane, O. Nasri, J. B. H. Slama, Interval-based solutions for reliable and safe navigation of intelligent autonomous vehicles, in: 2019 12th International Workshop on Robot Motion and Control (RoMoCo), 2019, pp. 124–130, Poznan, Poland.
- [31] JianglinLan, Ron J. Patton, "A new strategy for integration of fault estimation within fault-tolerant control", *Automatica*, Vol. 69, July 2016, Pages 48-59.
- [32] H. Jian, Z. Huaguang, W. Yingchun, and Z. Kun, "Fault Estimation and Fault-Tolerant Control for Switched Fuzzy Stochastic Systems", *IEEE TRANSACTIONS ON FUZZY SYSTEMS*, VOL. 26, NO. 5, OCTOBER 2018.
- [33] G. HUANG, SHE, Jinhua, FUKUSHIMA, F. Edwards, *et al.* Robust reconstruction of current sensor faults for PMSM drives in the presence of disturbances. *IEEE/ASME Transactions on Mechatronics*, 2019, vol. 24, no 6, p. 2919-2930.
- [34] J. Li, K. Pan, & Q. Su. (2019). *Sensor fault detection and estimation for switched power electronics systems based on sliding mode observer*. *Applied Mathematics and Computation*, 353, 282-294.
- [35] Z. Gong, D. Huang, H. U. K. Jadoon, L. Ma and W. Song, "Sensor-Fault-Estimation-Based Tolerant Control for Single-Phase Two-Level PWM Rectifier in Electric Traction System," in IEEE Trans on Power Electronics, vol. 35, no. 11, pp. 12274-12284, Nov. 2020
- [36] M. Merai, M. W. Naouar, I. S. Belkhdja and E. Monmasson, "An Adaptive PI Controller Design for DC-Link Voltage Control of Single-Phase Grid-Connected Converters," in IEEE Transactions on Industrial Electronics, vol. 66, no. 8, pp. 6241- 6249, Aug. 2019.
- [37] Y. Han, M. Luo, X. Zhao, J. Guerrero, L. Xu. *Comparative Performance Evaluation of Orthogonal-Signal-Generators-Based Single-Phase PLL Algorithms—A Survey*. IEEE Trans. Power Electron. 2016, 31, 3932–3944.
- [38] J. Xu, C. C. Mi, B. Cao, J. Deng, Z. Chen, and S. Li, "The State of Charge Estimation of Lithium-Ion Batteries Based on a Proportional-Integral Observer" in *IEEE Trans. Veh. Technol.*, vol. 63, no. 4, pp. 1614-1621, May 2014.